



Published in final edited form as:

Eur J Pharmacol. 2014 October 5; 740: 603–610. doi:10.1016/j.ejphar.2014.06.021.

Identification of novel small molecule modulators of K_{2P}18.1 two-pore potassium channel

J. Kyle Bruner^{a,b}, Beiyan Zou^{a,b}, Hongkang Zhang^{a,b}, Yixin Zhang^{a,b}, Katharina Schmidt^c, and Min Li^{a,b,*}

^aThe Solomon H. Snyder Department of Neuroscience, High Throughput Biology Center, Johns Hopkins University, Baltimore, MD 21205, USA

^bJohns Hopkins Ion Channel Center (JHICC), Johns Hopkins University, Baltimore, MD 21205, USA

^cDepartment of Physiology, Johns Hopkins University, Baltimore, MD 21205, USA

Abstract

Two-pore domain potassium (K_{2P}) channels are responsible for background potassium (K⁺) current, which is crucial for the maintenance of resting membrane potential. K_{2P}18.1, also called TWIK-related spinal cord K⁺ channel (TRESK) or KCNK18, is thought to be a major contributor to background K⁺ currents, particularly in sensory neurons where it is abundantly expressed. Despite its critical role and potential therapeutic implication, pharmacological tools for probing K_{2P}18.1 activity remain unavailable. Here, we report a high-throughput screen against a collection of bioactive compounds that yielded 26 inhibitors and 8 activators of K_{2P}18.1 channel activity with more than 10-fold selectivity over the homologous channel K_{2P}9.1. Among these modulators, the antihistamine loratadine inhibited K_{2P}18.1 activity with IC₅₀ of 0.49 ± 0.23 μM and is considerably more potent than existing K_{2P}18.1 inhibitors. Importantly, the inhibition by loratadine remains equally efficacious upon potentiation of K_{2P}18.1 by calcium signaling. Furthermore, the loratadine effect is dependent on transmembrane residues F145 and F352, providing orthogonal evidence that the inhibition is caused by a direct compound-channel interaction. This study reveals new pharmacological modulators of K_{2P}18.1 activity useful in dissecting native K_{2P}18.1 function.

Keywords

K_{2P}18.1; two-pore potassium channel; ion channels; small molecule drugs; high-throughput screens

© 2014 Elsevier B.V. All rights reserved.

*To whom correspondence should be addressed (ML: minli@jhmi.edu, 410.614.5131).

Publisher's Disclaimer: This is a PDF file of an unedited manuscript that has been accepted for publication. As a service to our customers we are providing this early version of the manuscript. The manuscript will undergo copyediting, typesetting, and review of the resulting proof before it is published in its final citable form. Please note that during the production process errors may be discovered which could affect the content, and all legal disclaimers that apply to the journal pertain.

1. Introduction

While many forms of cellular ionic current are dependent upon membrane voltage, K^+ background, or “leak”, current is voltage independent and crucial for maintenance of resting membrane potential. The molecules responsible for this background K^+ current are the two-pore domain potassium (K_{2P}) channels. The K_{2P} family currently consists of 15 members divided into six subfamilies (Enyedi and Czirjak, 2010).

$K_{2P}18.1$ (or TRESK) is a member of the K_{2P} family and resides in a subfamily of its own. $K_{2P}18.1$ stands apart from the other K_{2P} channels for several reasons, most prominently for its calcium-dependent augmentation. Unlike classical calcium-activated K^+ channels, calcium's effect is not caused by direct binding of calcium to the channel but via the activity of the serine/threonine phosphatase, calcineurin (Czirjak and Enyedi, 2006; Czirjak et al., 2004). Other proteins involved in regulation of $K_{2P}18.1$ include scaffolding 14-3-3 proteins and protein kinase A (Enyedi et al., 2012).

$K_{2P}18.1$ is found primarily in dorsal root ganglion (DRG) and trigeminal ganglion (TG) neurons and was reported to be a major contributor to background current in DRG neurons (Kang and Kim, 2006; Lafreniere et al., 2010). In addition to its important roles in peripheral sensory neurons, human genetics studies have recently shown that a dominant-negative mutation in $K_{2P}18.1$ found in patients is directly linked to familial migraine with aura (Lafreniere et al., 2010). This mutation was shown to induce neuronal hyperexcitability when expressed in TG neurons (Liu et al., 2013). These studies contribute to emerging evidence that $K_{2P}18.1$ plays an important role in pain-related disorders, and raise the possibility of developing $K_{2P}18.1$ modulators to achieve therapeutic benefits.

To date, several compounds are known to have $K_{2P}18.1$ modulatory activity (Kang et al., 2008; Tulleuda et al., 2011). Like many K_{2P} channels, $K_{2P}18.1$ activity is enhanced by application of volatile anesthetics such as isoflurane. The local anesthetic lidocaine was shown to inhibit human $K_{2P}18.1$ with half-maximal inhibitory concentration (IC_{50}) of 3.4 mM (Liu et al., 2004). In addition, two compounds appear to display certain selectivity for $K_{2P}18.1$ over other K_{2P} family members. The sodium channel blocker lamotrigine was shown to inhibit mouse $K_{2P}18.1$ specifically over $K_{2P}10.1$ with an IC_{50} of 47 μ M (Kang et al., 2008). Isobutylalkenyl amide (IBA), a derivative of hydroxyl- α -sanshool, was shown to inhibit mouse $K_{2P}18.1$ by approximately 70% at a concentration of 500 μ M but displayed no inhibitory activity against $K_{2P}2.1$, $K_{2P}10.1$, or $K_{2P}4.1$ at this concentration (Tulleuda et al., 2011).

The purpose of this study was to search for better small-molecule modulators of $K_{2P}18.1$ that directly target the channel. This was pursued by first screening the Library of Pharmacologically Active Compounds (LOPAC) against the $K_{2P}18.1$ channel using a fluorescent-based assay. This was followed by a counter screen to separate compounds with or without activity against the homologous channel $K_{2P}9.1$. Compounds of sufficient selectivity and potency were then chosen for further validation and characterization using both the fluorescent-based assay and electrophysiology. Critical residues for conferring drug sensitivity were investigated using wild type and mutant channels.

2. Materials and Methods

2.1 Cell Culture and Transfection

HEK293 cells were grown in Dulbecco's Modified Eagle Medium (DMEM) supplemented with 10% fetal bovine serum (FBS) and 2 mM L-Glutamine. HEK293-K₂p9.1 stable cell lines were previously generated (Miller et al., 2012) and K₂p9.1 expression was induced by incubation with 1 μ M tetracycline for 16 h. These cells were cultured in DMEM supplemented with 10% FBS, 2 mM L-Glutamine, 400 μ g/ml hygromycin, and 15 μ g/ml blasticidin. All cells were maintained at 37°C in 5% CO₂.

To express K₂p18.1 channels (encoded by the *KCNK18* gene), HEK293 cells were transfected using either FuGENE 6[®] transfection reagent (Promega, Madison WI) or via electroporation using the MaxCyte platform. Cells were transfected with both human K₂p18.1 cDNA (OriGene Technologies, Rockville, MD) and either GFP or mCherry. Experiments were performed 24–48 h after transfection.

2.2 Compounds

All compounds for the primary screening and follow-up analysis were purchased from Sigma-Aldrich (St. Louis, MO). The Library of Pharmacologically Active Compounds (LOPAC) consists of 1,280 small molecules with well-characterized biological activities. The library was kept at 10 mM in DMSO. Loratadine (4-(8-Chloro-5,6-dihydro-11H-benzo[5,6]cyclohepta[1,2-b]pyridin-11-ylidene-1-piperidinecarboxylic acid ethyl ester) and carbachol (carbamoylcholine chloride, (2-Hydroxyethyl)trimethyl-ammonium chloride carbamate) were dissolved in DMSO to a stock concentration of 50 mM. Lidocaine (2-Diethylamino-N-(2,6-dimethylphenyl)acetamide) was dissolved in saline to a stock concentration of 200 mM.

2.3 Thallium-Flux Assays

For the primary screen, HEK293 cells transfected with human K₂p18.1 were used. Un-transfected cells served as a negative control. An equal number of cells (7,000 cells/50 μ l) were added to each well of 384-well assay plates (BD polylysine-precoated, San Jose, CA). Cells were maintained at 37°C in 5% CO₂ for 18 h before the assay. For assay, cells were loaded with FluxOR[™] Tl⁺-sensitive dye (Life Technologies, Grand Island, NY) for 90 min in the dark at room temperature. Following this, dye containing buffer was replaced with a buffer containing 1X Hank's balanced salt solution (with Ca²⁺ and Mg²⁺), 20 mM HEPES, and 0.77 mg/ml probenecid. Library compounds were added 20 min prior to Tl⁺ stimulation. The plate was loaded onto a FDSS 6000 (Hamamatsu, Middlesex, NJ) and a baseline was established after 10 s fluorescent signal detection. Then, 5X stimulus buffer containing 1X chloride-free buffer (Life Technologies), 25mM K₂SO₄, and 7.5mM Tl₂SO₄ was added, and fluorescence signal continued to be detected for 140 s. The counter screen utilized the same assay technique as reported (Miller et al., 2012) with tetracycline induced HEK293-K₂p9.1 cells plated at 15,000 cells/50 μ l. Transfected or induced cells stimulated with buffer only were used as positive controls. Un-transfected or noninduced cells stimulated with buffer only were used as negative controls. To evaluate assay quality, Z' factor was calculated as

described (Zhang et al., 1999) using fluorescence intensity at 100 s for inhibitors and 50 s for activators.

Potential inhibitory effect was assessed by measuring the fluorescence intensity at 100 s and potential activation effect was assessed by measuring fluorescence intensity at 50 s (see Fig. S2). Fluorescence change was calculated and activity was normalized using the B scores method as reported (Brideau et al., 2003) to evaluate compound effects. Compared to buffer controls, a compound that caused more than 2.25 S.D. increase in activity was defined as an activator; a compound that caused more than 3 S.D. reduction in activity was defined as an inhibitor.

In the validation assays, compounds were tested in a 10-point 1:3 gradient in quadruplicate with the highest concentration at 30 μ M. In the characterization assays, lidocaine was tested in a 10-point 1:2 gradient in triplicate and loratadine was tested in a 10-point 1:3 gradient in quadruplicate with the highest concentrations at 20 mM and 150 μ M respectively.

2.4 Site-directed Mutagenesis

Mutant K_{2p}18.1 (mutK_{2p}18.1) was generated using a QuikChange Lightning site-directed mutagenesis kit (Agilent Technologies, Santa Clara, CA) according to the provided protocol. F145A/F352A double mutant was generated from successive single mutations and mutant K_{2p}18.1 DNA was confirmed by sequencing.

2.5 Manual Electrophysiological Studies

HEK293 cells heterologously expressing wild type K_{2p}18.1 (HEK293-wtK_{2p}18.1), those expressing mutant K_{2p}18.1 (HEK293-mutK_{2p}18.1), or those expressing K_{2p}9.1 (HEK293-K_{2p}9.1) were seeded onto poly-L-lysine coated coverslips one day before recordings were performed. For cells transfected with K_{2p}18.1, only cells expressing GFP or mCherry were selected for recording. Pipettes were pulled from micropipette glass (World Precision Instruments Inc., Sarasota, FL) to 2–4 M Ω when filled with a pipette solution containing 145 mM KCl, 1 mM MgCl₂, 10 mM HEPES, 5 mM EGTA, 5 mM MgATP, pH 7.25 and placed in a bath solution containing 140 mM NaCl, 5 mM KCl, 2 mM CaCl₂, 1.5 mM MgCl₂, 10 mM HEPES, 10 mM Glucose, pH 7.35. Isolated cells were voltage-clamped in the whole-cell configuration using a patch clamp amplifier Axopatch 200B (Molecular Devices, Sunnyvale, CA). Currents were filtered at 1 kHz, digitized at 10 kHz, and acquired with pClamp 9 software. The holding potential was –80 mV. The voltage protocol consisted of a 50 ms step to –120 mV, a 500 ms ramp from –120 mV to +60 mV, a 500 ms step to –80 mV, and finally a 500 ms step to +60 mV. This protocol was repeated every 5 s.

Representative current traces were taken from the 500 ms ramp. Current was measured at the end of the +60 mV step to determine extent of compound inhibition. Data was analyzed with Clampfit 9 (Molecular Devices).

2.6 Statistical analyses

Sigmoidal fitting, linear fitting, and EC₅₀/IC₅₀ value determination were performed using Origin 6.0 (OriginLab, Northampton, MA). Data are expressed as mean \pm S.D. Statistical significance was determined using Student's t-test for independent samples.

3. Results

3.1 Screening for Specific Modulators of K_{2p}18.1 Channel Activity

As most K⁺ channels are permeable to TI⁺, pre-loading with a fluorescent TI⁺-sensitive dye allows for an increase in intracellular TI⁺ concentration to be used as a surrogate readout of channel activity with attractive signal to noise ratio (Weaver et al., 2004). Using a commercial fluorescence-based TI⁺ flux assay, the bioactive LOPAC collection compounds were tested at 10 μ M in duplicate against HEK293 cells expressing human K_{2p}18.1 (HEK293-K_{2p}18.1) to look for small-molecule modulators of K_{2p}18.1 channel activity. A good correlation was observed between replicates with $R = 0.96$ (Fig. S1) and Z' factors of 0.79 ± 0.05 for activators and 0.79 ± 0.04 for inhibitors. The assay is therefore of sufficient quality for reliable hit identification. Compared to buffer controls, compounds that increased fluorescence intensity by more than 2.25 S.D. were selected as activator hits while those that decreased fluorescence intensity by more than 3 S.D. were selected as inhibitor hits. Based on these criteria, the hit rate was 0.94% for activators and 2.19% for inhibitors. In order to profile target selectivity of active compounds, a parallel counter screen was performed using the same library under identical conditions against HEK293 cells expressing human K_{2p}9.1 (HEK293-K_{2p}9.1). Compound activity against both K_{2p} channels was compared and is plotted in Fig. 1B and 1C. Those compounds with preference for K_{2p}18.1 were selected for further validation. Experimental outline is diagramed in Fig. 1A.

3.2 Validation of Compound Activity and Determination of Potency and Efficacy

To confirm the activity of the selected compounds and to estimate their potency, a validation assay was performed on all K_{2p}18.1-selective compounds. We tested concentrations ranging from 1.5 nM to 30 μ M for each compound against both HEK293-K_{2p}18.1 cells and HEK293-K_{2p}9.1 cells. The potencies and efficacies of all activators and inhibitors are summarized in Table 1 and Table 2. In total, 26 inhibitors and 8 activators were confirmed with half maximal effective concentration below 30 μ M and better than 10-fold specificity for K_{2p}18.1 over K_{2p}9.1.

The identified inhibitors are bioactive and some are known to have diverse activities. Fig. 2 shows the structures of these active compounds, which include the antibiotic oligomycin A ($IC_{50}=3.71 \pm 0.82$ μ M), the CB2 cannabinoid receptor agonist JWH-015 ($IC_{50}=5.47 \pm 0.37$ μ M), the thromboxane A2 receptor antagonist L-655,240 ($IC_{50}=7.35 \pm 0.47$ μ M), and the antihistamine loratadine ($IC_{50}=0.69 \pm 0.06$ μ M). Few identified inhibitors have any connection to each other in terms of their known mechanisms of action, and none have been previously shown to have any activity against K_{2p}18.1 (Hall et al., 1987; Kreutner W, 1987; Lombard et al., 2007; Salomon AR, 2001). Among the inhibitors, the antihistamine loratadine displayed considerable potency and selectivity and was therefore chosen for further characterization studies to explore its mechanism of action.

3.3 Characterization of Loratadine Activity on K_{2p}18.1

To investigate the activity of loratadine on K_{2p}18.1, we compared its pharmacological characteristics with that of a known, but non-selective, K_{2p}18.1 pore blocker, lidocaine (Kim et al., 2013; Liu et al., 2004). We first tested whether loratadine may exert its effects

via modulation of receptor signaling pathways, consequently down-regulating channel activity. We employed a Ti^+ flux assay to determine the effects of inhibitors in the presence and absence of carbachol, which activates $\text{K}_{2\text{p}}18.1$ via its activation effect on endogenous muscarinic G-protein coupled receptors in HEK293 cells (Table 2 and Luo et al., 2008). In these experiments, $30\mu\text{M}$ carbachol, a concentration known to activate $\text{K}_{2\text{p}}18.1$ activity, was employed to turn on endogenous M receptors (Braun et al., 2011). Thallium-induced fluorescent responses were recorded, and the signal intensity was normalized to give rise to concentration-response curves (Fig. 3). The IC_{50} values for lidocaine with and without carbachol were $3.41 \pm 0.57 \text{ mM}$ and $3.65 \pm 0.38 \text{ mM}$, respectively. These results are consistent with previously reported values for lidocaine activity and with its pore blocking mechanism (Kim et al., 2013; Liu et al., 2004). The IC_{50} values for loratadine with and without carbachol were $0.66 \pm 0.02 \mu\text{M}$ and $0.69 \pm 0.06 \mu\text{M}$, respectively. As with lidocaine, loratadine showed virtually identical potencies and efficacies independent of channel activation. These data argue favorably that the primary action of loratadine, similar to lidocaine, is not through modulating a signaling pathway to down regulate the channel activity but rather through a direct interaction with $\text{K}_{2\text{p}}18.1$ channels.

Admittedly, G-protein coupled receptor signaling is one of several pathways that could modulate $\text{K}_{2\text{p}}18.1$ activity and the Ti^+ -based flux measurement applied here is an endpoint, accumulative readout. In order to more directly monitor compound effects on ionic current, activity of recombinantly expressed $\text{K}_{2\text{p}}18.1$ in HEK293 cells was measured using whole-cell patch clamp recording in compound-free conditions and in the presence of either 1 mM lidocaine or $10 \mu\text{M}$ loratadine. The membrane potential of cells was held at -80 mV , followed by a ramp from -120 mV to $+60 \text{ mV}$ over a duration of 500 ms , then a step to $+60 \text{ mV}$. Un-transfected cells showed small background currents ($<200 \text{ pA}$ at $+60 \text{ mV}$, data not shown). However, transfected cells resulted in large currents ($>1,000 \text{ pA}$ at $+60 \text{ mV}$, Fig. 4A) with outward rectification. Fig. 4A shows representative traces of the ramp protocol from cells exposed to each compound. 1 mM lidocaine and $10 \mu\text{M}$ loratadine inhibited wild type $\text{K}_{2\text{p}}18.1$ (wt $\text{K}_{2\text{p}}18.1$) by $65.2 \pm 10.4\%$ ($n=5$) and $87.5 \pm 3.7\%$ ($n=5$), respectively. Loratadine was then tested at 3 more concentrations, $0.1 \mu\text{M}$, $1 \mu\text{M}$, and $50 \mu\text{M}$ to test its concentration-dependent effects (Fig. 4C). The IC_{50} of loratadine against $\text{K}_{2\text{p}}18.1$ was $0.49 \pm 0.23 \mu\text{M}$ ($n=4$). To validate its selectivity for $\text{K}_{2\text{p}}18.1$, loratadine was tested at the same concentrations against $\text{K}_{2\text{p}}9.1$ using tetracycline induced HEK293- $\text{K}_{2\text{p}}9.1$ cells (Fig. 4C). The IC_{50} of loratadine against $\text{K}_{2\text{p}}9.1$ was $5.27 \pm 1.69 \mu\text{M}$ ($n=4$), indicating ~ 11 -fold selectivity for $\text{K}_{2\text{p}}18.1$.

3.4 Molecular Determinants Critical for $\text{K}_{2\text{p}}18.1$ Sensitivity to Loratadine

Structural modeling has been performed for mouse $\text{K}_{2\text{p}}18.1$ and was used to determine key residues for inhibitory activity of multiple known, nonspecific $\text{K}_{2\text{p}}18.1$ inhibitors including lidocaine (Kim et al., 2013). The two residues identified as important for inhibition were F156 and F364, which are present in the 2nd and 4th transmembrane domains of $\text{K}_{2\text{p}}18.1$ respectively. In human $\text{K}_{2\text{p}}18.1$, the corresponding residues, F145 and F352, are conserved. To determine whether these residues are also critical for lidocaine inhibition on human $\text{K}_{2\text{p}}18.1$, and to examine whether loratadine activity is dependent on these residues, the

effects of lidocaine and loratadine were examined on the F145A/F352A double mutant K_{2p}18.1 (mutK_{2p}18.1).

First, the non-selective K_{2p}18.1 blocker lidocaine was used to determine the importance of the F145 and F352 residues for inhibitor activity. Similar to the mouse K_{2p}18.1 mutant, the human mutant formed functional channels when expressed in HEK293 cells. The TI⁺ flux assay revealed a rightward shift of the IC₅₀ to 11.6 ± 7.1 mM for lidocaine against mutK_{2p}18.1 (Fig. 4E). Whole-cell patch clamp recording showed a significant reduction in lidocaine effectiveness against mutK_{2p}18.1 compared to wild type, with 1 mM lidocaine inhibiting mutK_{2p}18.1 current by only $18.2 \pm 5.8\%$ (Fig. 4, B and D, n=5). This is in agreement with earlier data in which F156A/F364A double mutant mouse K_{2p}18.1 was inhibited by 1 mM lidocaine only $20 \pm 15\%$, significantly less than the $83 \pm 5\%$ inhibition of the wild type channel (Kim et al., 2013), and confirms the role of the F145 and F352 residues of human K_{2p}18.1 for lidocaine activity.

Next, mutK_{2p}18.1 was used to establish whether loratadine's inhibitory activity is also dependent on the F145 and F352 residues. When measured in the TI⁺ flux assay, loratadine failed to reach 50% inhibition against mutK_{2p}18.1 at the maximally tested concentration of 150 μ M, suggesting at least 50 fold lower potency compared to wtK_{2p}18.1 (Fig. 4F). Whole-cell patch clamp recording further validated a significantly reduced inhibition, with 10 μ M loratadine inhibiting mutK_{2p}18.1 current by $3.9 \pm 13.3\%$ (Fig. 4, B and D, n=4). Taken together, these data demonstrate that the F145 and F352 residues on human K_{2p}18.1 are among key molecular determinants for the inhibitory activity of loratadine.

4. Discussion

The *KCNK18* gene was first cloned in 2003 from human spinal cord (Sano et al., 2003). At the time, the K_{2p}18.1 channel was identified as a member of the K_{2p} family expressed in the spinal cord with low sequence similarity yet somewhat comparable pharmacology to other family members. More recently, K_{2p}18.1 gained considerable interest when a dominant-negative mutation in *KCNK18* was directly linked to a subset of patients with familial migraine with aura. However, K_{2p}18.1 physiology in native systems is still poorly understood, and one of the roadblocks to advancing this understanding lies with the lack of quality pharmacological tools for probing its activity.

Here we developed an effective assay and screened the commercially available library of bioactive compounds (LOPAC) to search for modulators of K_{2p}18.1 channel activity. To gain an initial insight into specificity for K_{2p}18.1, this library was also screened against another member of the K_{2p} family, K_{2p}9.1. From the identified hits, 26 inhibitors and 8 activators were verified with selectivity for K_{2p}18.1 over K_{2p}9.1. Admittedly, to better characterize the specificity one important future direction is to establish its selectivity profile by systematically testing these compounds against a range of other targets including but not limited to other K_{2p} family members. Of note, a sequence alignment of all 15 K_{2p} family members reveals that the F145 and F352 residues on K_{2p}18.1 critical for inhibition by loratadine are completely unique to K_{2p}18.1 (Fig. S3). The K_{2p}18.1-specific residues critical

for drug sensitivity provide a plausible molecular explanation for specificity for K_{2p}18.1 over K_{2p}9.1 as reported here, and may hold true for other family members in future studies.

Among the identified activators, six have reported muscarinic acetylcholine receptor agonist activity. As K_{2p}18.1 is calcium-activated, these compounds are very likely activating K_{2p}18.1 via stimulation of endogenous M₃ muscarinic acetylcholine receptors present on HEK293 cells (Pierce et al., 2002; Luo et al., 2008). Another identified activator, spiperone hydrochloride, is known to elevate intracellular calcium levels in HEK293 cells (Lu and Carson, 2009). Phorbol 12-myristate 13-acetate (PMA) is an activator of protein kinase C and has been previously shown to activate K_{2p}18.1 through kinase activity (Rahm et al., 2012). Other interesting compounds include those that appear to have higher selectivity for K_{2p}9.1 (Fig. 1C). Some compounds seem to activate K_{2p}9.1 yet inhibit or have no effect on K_{2p}18.1. These actives, while not in the scope of the present studies, are worth further characterization in future investigations.

In addition to the identification of a series of tool compounds, this work has also begun to provide insights into the mechanism of action by the antihistamine loratadine. The effects of loratadine were examined using the TI⁺ flux assay and patch clamp recording. The recording protocol was adapted from the literature for proper comparison of compound pharmacology. The ramp from -120 mV to +60 mV allowed for visualization of characteristic K_{2p}18.1 outward rectification and assessment of recording quality, while the step to +60 mV provided sufficient time resolution for accurate measurement and quantification. Only recordings with current amplitude 1000 pA at +60 mV and a consistent reversal potential near the expected -85mV were used for analysis. It is important to note that the TI⁺ flux assay and patch clamp recording yielded comparable IC₅₀ values with respect to loratadine inhibition, which argues for the validity of the TI⁺ based high throughput screening assay. This compatibility therefore justifies future use of this assay for larger HTS campaigns to discover other chemical structures with suitable pharmacology and drugability.

Both loratadine and the known K_{2p}18.1 blocker lidocaine showed equal levels of modulatory activity independent of channel activation by carbachol-induced signaling. This suggests that loratadine, regardless of its mechanism of action, is acting downstream from the carbachol pathway. Based on a homology model, two key residues, F156 and F364 in mouse K_{2p}18.1 and conserved as F145 and F352 in human K_{2p}18.1, have been shown to face the central cavity and interact with the K_{2p}18.1 blockers quinine, propafenone, and lidocaine via π - π interactions (Kim et al., 2013). Mutating these residues to alanine in mouse K_{2p}18.1 resulted in diminished inhibition by all three compounds. In this study, we generated the equivalent mutant human K_{2p}18.1 channel, F145A/F352A. Indeed, lidocaine showed significantly reduced inhibitory activity against the mutant channel. Loratadine showed an even more dramatic reduction in activity against the mutant as compared to wild type. The differential extents affected by the mutation may be the molecular basis for the target selectivity. Based on the earlier modeling and the data here, a plausible model would involve F145 and F352 residues being the key residues for mediating binding of K_{2p}18.1 inhibitors including loratadine. The mechanism of loratadine is less likely through allosteric effects but rather a direct block of the permeation pathway. While more work is needed to understand the mechanism of interaction and specificity, based on its pharmacology reported

here, loratadine is significantly more potent than both lamotrigine and isobutylalkenyl amide (IBA), suggesting it may serve as a more effective inhibitor probe of K_{2p}18.1 activity. Although loratadine has been shown to inhibit other potassium channels, including human ether-a-go-go-related gene (hERG) and Kv1.5, it would certainly serve as a useful tool in DRG and TG neurons where K_{2p}18.1 is most abundantly expressed (Kang and Kim, 2006; Lafreniere et al., 2010; Lacerda et al., 1997; Crumb, 2000).

In summary, we report the identification and validation of several small molecules that modulate K_{2p}18.1 channel activity specifically over K_{2p}9.1. In particular, a large number of channel inhibitors were identified, at least one of which likely directly blocks the channel pore. Furthermore, two residues, F145 and F352, specifically conserved in K_{2p}18.1, are key determinants for drug sensitivity. The compounds identified here may be useful for probing native K_{2p}18.1 in order to identify its precise physiological role.

Supplementary Material

Refer to Web version on PubMed Central for supplementary material.

Acknowledgments

We thank members of the Li laboratory for valuable discussions and comments on the manuscript and Alison Neal for editorial assistance. This work was supported by National Institutes of Health and MLPCN grants RO1GM078579, U54MH084691 (M.L.). Johns Hopkins University is a member of the MLPCN and houses the Johns Hopkins Ion Channel Center.

References

- Braun G, Nemcsics B, Enyedi P, Czirjak G. TRESK background K(+) channel is inhibited by PAR-1/ MARK microtubule affinity-regulating kinases in *Xenopus* oocytes. *PloS one*. 2011; 6:e28119. [PubMed: 22145024]
- Brideau C, Gunter B, Pikounis B, Liaw A. Improved statistical methods for hit selection in high-throughput screening. *Journal of biomolecular screening*. 2003; 8:634–647. [PubMed: 14711389]
- Crumb WJ. Loratadine blockade of K⁺ channels in human heart: comparison with terfenadine under physiological conditions. *Journal of pharmacology and experimental therapeutics*. 2000; 292:261–264.
- Czirjak G, Enyedi P. Targeting of calcineurin to an NFAT-like docking site is required for the calcium-dependent activation of the background K⁺ channel, TRESK. *The Journal of biological chemistry*. 2006; 281:14677–14682. [PubMed: 16569637]
- Czirjak G, Toth ZE, Enyedi P. The two-pore domain K⁺ channel, TRESK, is activated by the cytoplasmic calcium signal through calcineurin. *The Journal of biological chemistry*. 2004; 279:18550–18558. [PubMed: 14981085]
- Enyedi P, Braun G, Czirjak G. TRESK: the lone ranger of two-pore domain potassium channels. *Molecular and cellular endocrinology*. 2012; 353:75–81. [PubMed: 22115960]
- Enyedi P, Czirjak G. Molecular background of leak K⁺ currents: two-pore domain potassium channels. *Physiological reviews*. 2010; 90:559–605. [PubMed: 20393194]
- Hall RA, Gillard J, Guindon Y, Letts G, Champion E, Ethier D, Evans J, Ford-Hutchinson AW, Fortin R, Jones TR, Lord A, Morton HE, Rokach J, Yoakim C. Pharmacology of L-655,240 (3-[1-(4-chlorobenzyl)-5-fluoro-3-methyl-indol-2-yl]2,2-dimethylpropanoic acid); a potent, selective thromboxane/prostaglandin endoperoxide antagonist. *European Journal of Pharmacology*. 1987; 135:193–201. [PubMed: 3582493]

- Kang D, Kim D. TREK-2 (K2P10.1) and TRESK (K2P18.1) are major background K⁺ channels in dorsal root ganglion neurons. *American journal of physiology. Cell physiology*. 2006; 291:C138–146. [PubMed: 16495368]
- Kang D, Kim GT, Kim EJ, La JH, Lee JS, Lee ES, Park JY, Hong SG, Han J. Lamotrigine inhibits TRESK regulated by G-protein coupled receptor agonists. *Biochemical and biophysical research communications*. 2008; 367:609–615. [PubMed: 18190784]
- Kim S, Lee Y, Tak HM, Park HJ, Sohn YS, Hwang S, Han J, Kang D, Lee KW. Identification of blocker binding site in mouse TRESK by molecular modeling and mutational studies. *Biochimica et biophysica acta*. 2013; 1828:1131–1142. [PubMed: 23200789]
- Kreutner W, Chapman RW, Gulbenkian A, Siegel MI. Antiallergic activity of loratadine, a non-sedating antihistamine. *Allergy*. 1987; 42:57–63. [PubMed: 2436504]
- Lacerda AE, Roy ML, Lewis EW, Rampe D. Interactions of the nonsedating antihistamine loratadine with a Kv1.5-type potassium channel cloned from human heart. *Molecular pharmacology*. 1997; 52:314–322. [PubMed: 9271355]
- Lafreniere RG, Cader MZ, Poulin JF, Andres-Enguix I, Simoneau M, Gupta N, Boisvert K, Lafreniere F, McLaughlan S, Dube MP, Marcinkiewicz MM, Ramagopalan S, Ansorge O, Brais B, Sequeiros J, Pereira-Monteiro JM, Griffiths LR, Tucker SJ, Ebers G, Rouleau GA. A dominant-negative mutation in the TRESK potassium channel is linked to familial migraine with aura. *Nature medicine*. 2010; 16:1157–1160.
- Liu C, Au JD, Zou HL, Cotten JF, Yost CS. Potent activation of the human tandem pore domain K channel TRESK with clinical concentrations of volatile anesthetics. *Anesthesia and analgesia*. 2004; 99:1715–1722. [PubMed: 15562060]
- Liu P, Xiao Z, Ren F, Guo Z, Chen Z, Zhao H, Cao YQ. Functional analysis of a migraine-associated TRESK K⁺ channel mutation. *The Journal of neuroscience: the official journal of the Society for Neuroscience*. 2013; 33:12810–12824. [PubMed: 23904616]
- Lombard C, Nagarkatti M, Nagarkatti P. CB2 cannabinoid receptor agonist, JWH-015, triggers apoptosis in immune cells: potential role for CB2-selective ligands as immunosuppressive agents. *Clinical immunology*. 2007; 122:259–270. [PubMed: 17185040]
- Lu D, Carson DA. Spiperone enhances intracellular calcium level and inhibits the Wnt signaling pathway. *BMC pharmacology*. 2009; 9:13. [PubMed: 19948059]
- Luo J, Busillo JM, Benovic JL. M3 muscarinic acetylcholine receptor-mediated signaling is regulated by distinct mechanisms. *Molecular pharmacology*. 2008; 74:338–347. [PubMed: 18388243]
- Miller, MR.; Zou, B.; Shi, J.; Flaherty, DP.; Simpson, DS.; Yao, T.; Maki, BE.; Day, VW.; Douglas, JT.; Wu, M.; McManus, OB.; Golden, JE.; Aubé, J.; Li, M. Probe Reports from the NIH Molecular Libraries Program [Internet]. Bethesda (MD): National Center for Biotechnology Information (US); Apr 16. 2010 2012 Development of a Selective Chemical Inhibitor for the Two-Pore Potassium Channel, KCNK9. [Updated 2013 Feb 28] Available from: <http://www.ncbi.nlm.nih.gov/books/NBK133427/>
- Pierce KL, Premont RT, Lefkowitz RJ. Seven-transmembrane receptors. *Nature reviews. Molecular cell biology*. 2002; 3:639–650. [PubMed: 12209124]
- Rahm AK, Gierten J, Kisselbach J, Staudacher I, Staudacher K, Schweizer PA, Becker R, Katus HA, Thomas D. PKC-dependent activation of human K(2P) 18.1 K(+) channels. *British journal of pharmacology*. 2012; 166:764–773. [PubMed: 22168364]
- Salomon AR, Voehringer DW, Herzenberg LA, Khosla C. Apoptolidin, a selective cytotoxic agent, is an inhibitor of F0F1-ATPase. *Chemistry & Biology*. 2001; 8:71–80. [PubMed: 11182320]
- Sano Y, Inamura K, Miyake A, Mochizuki S, Kitada C, Yokoi H, Nozawa K, Okada H, Matsushime H, Furuichi K. A novel two-pore domain K⁺ channel, TRESK, is localized in the spinal cord. *The Journal of biological chemistry*. 2003; 278:27406–27412. [PubMed: 12754259]
- Tulleuda A, Cokic B, Callejo G, Saiani B, Serra J, Gasull X. TRESK channel contribution to nociceptive sensory neurons excitability: modulation by nerve injury. *Molecular pain*. 2011; 7:30. [PubMed: 21527011]
- Weaver CD, Harden D, Dworetzky SI, Robertson B, Knox RJ. A thallium-sensitive, fluorescence-based assay for detecting and characterizing potassium channel modulators in mammalian cells. *Journal of biomolecular screening*. 2004; 9:671–677. [PubMed: 15634793]

Zhang JH, Chung DY, Oldenberg KR. A simple statistical parameter for use in evaluation and validation of high throughput screening assays. *Journal of biomolecular screening*. 1999; 4:67–73. [PubMed: 10838414]

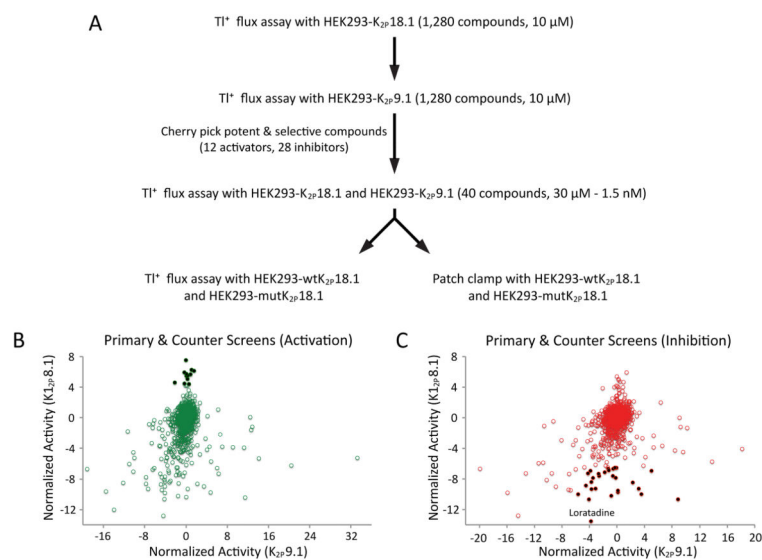


Fig. 1. Identification of K_{2p}18.1 modulators by a thallium based screening of LOPAC. (A) Flowchart outlining the screening and characterization process. (B) and (C) Scatter plots showing the results of the primary and counter screens for activators (B) and inhibitors (C) of K_{2p}18.1 channel activity. Normalized activity against both K_{2p}18.1 and K_{2p}9.1 at 100 s (inhibitors) or 50 s (activators) is plotted. Filled circles indicate compounds chosen for validation assay. Loratadine is labeled.

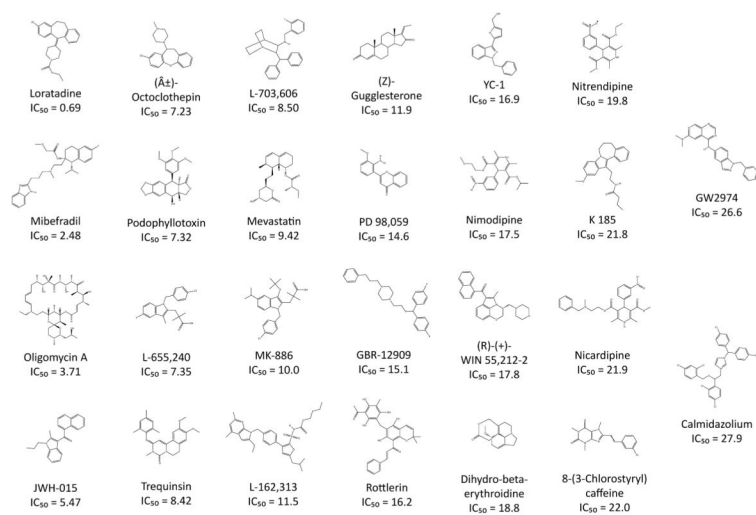


Fig. 2.
Structures and potencies of identified $K_{2p18.1}$ inhibitors.

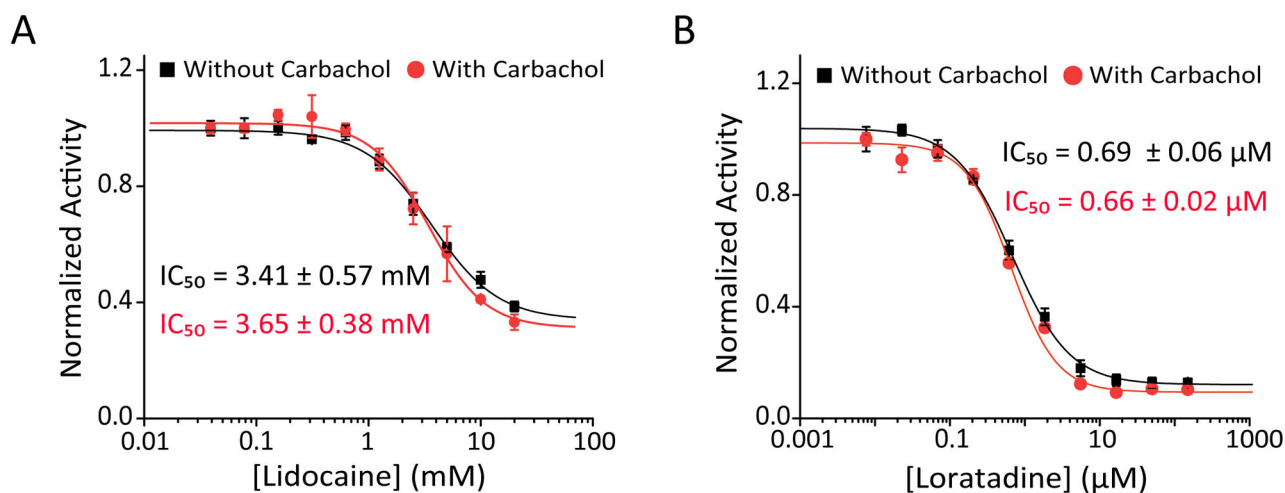
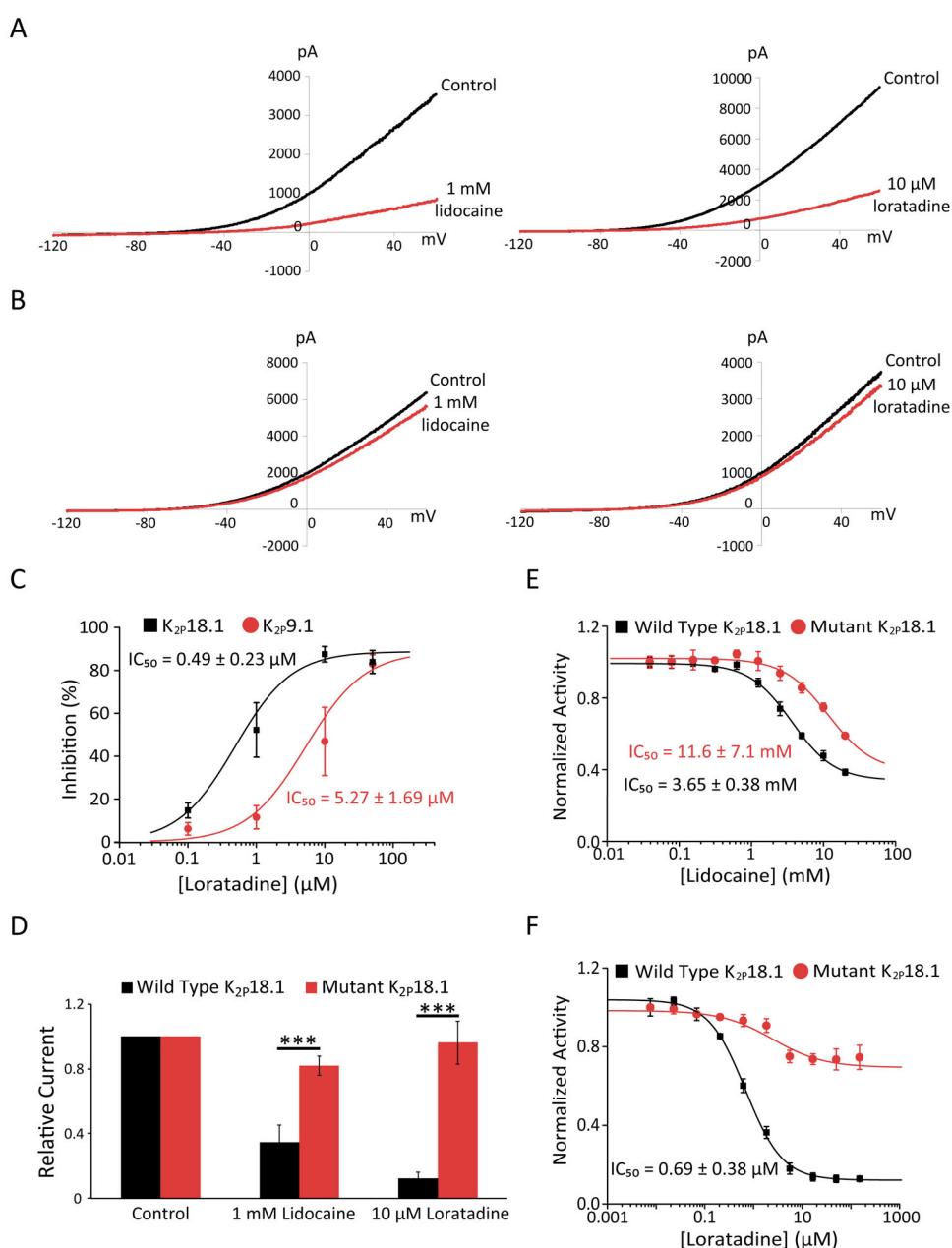


Fig. 3. Lidocaine and loratadine inhibit $K_{2p18.1}$ channel activity independent of activation state. (A) and (B) Concentration-response curves for $K_{2p18.1}$ inhibition by lidocaine (A) and loratadine (B) as measured in the presence and absence of 30 μ M carbachol. Fluorescence intensity was measured as a readout of TI^+ flux. Each curve was normalized to the value of the lowest compound concentration. Each point is mean \pm S.D. $n = 4$ for both compounds.

**Fig. 4.**

Comparison of K_{2p}18.1 inhibitors on the wild type and mutant channels. (A) and (B) Representative traces for inhibition of wtK_{2p}18.1 (A) and mutK_{2p}18.1 (B) by lidocaine and loratadine. The holding potential for recording was -80 mV and K_{2p}18.1 current was elicited by a ramp protocol from -120 mV to +60 mV. (C) Concentration-response inhibition of loratadine on wtK_{2p}18.1 and K_{2p}9.1 activity. Currents amplitudes were measured at +60 mV. Each point is mean ± S.D. of 4 measurements. (D) Summary of wtK_{2p}18.1 and mutK_{2p}18.1 inhibition by lidocaine and loratadine. Currents were measured at +60 mV. Each bar is mean ± S.D. of 4 measurements. *** indicates statistical significance (P < 0.001) (E) and (F) Concentration-response curves for wtK_{2p}18.1 and

mutK_{2p18.1} inhibition by lidocaine (E) and loratadine (F). Fluorescence intensity was measured as a readout of Tl⁺ flux. Each curve was normalized to the value of the lowest compound concentration. n = 3 for lidocaine, n = 4 for loratadine.

Table 1

Potency and Efficacy Values from Validation Assay for Validated K_{2p}18.1 Inhibitors

Compound Name	Reported Biological Activity	K _{2p} 18.1 IC ₅₀ (μM)	K _{2p} 18.1 Minimum Activity (%)	K _{2p} 9.1 IC ₅₀ (μM)	K _{2p} 9.1 Minimum Activity (%)
Loratadine	H1 Histamine receptor antagonist	0.69 (± 0.38)	0 (fixed)	63.4 (± 39.6)	0 (fixed)
Mibefradil dihydrochloride	T-type Ca ²⁺ Channel Blocker	2.48 (± 0.35)	11.9 (± 2.04)	24.6 (± 217)	72.0 (± 347)
Oligomycin A	Mitochondrial F ₀ F ₁ -ATP synthase inhibitor; antibiotic	3.71 (± 0.82)	52.0 (± 4.21)	47.7 (± 6.77)	0 (fixed)
JWH-015	Selective CB2 cannabinoid receptor agonist	5.47 (± 0.37)	26.7 (± 2.1)	≥ 30	-
(±)-Octothepin maleate	D2 Dopamine receptor antagonist; serotonin receptor antagonist	7.23 (± 0.95)	0 (fixed)	73.8 (± 20.4)	0 (fixed)
Podophyllotoxin	Antineoplastic glucoside; inhibitor of microtubule assembly	7.32 (± 0.54)	0 (fixed)	≥ 30	-
L-655,240	Thromboxane A2 (TXA2) receptor antagonist	7.35 (± 0.47)	0 (fixed)	≥ 30	-
Trequinsin hydrochloride	Phosphodiesterase III (PDE III) inhibitor	8.42 (± 4.63)	3.90 (± 20.2)	≥ 30	-
L-703,606 oxalate	Potent and selective NK1 tachykinin receptor antagonist	8.50 (± 2.13)	1.30 (± 9.2)	45.5 (± 337)	44.1 (± 395)
Mevastatin	Antibiotic	9.24 (± 1.63)	13.7 (± 7.6)	159 (± 154)	0 (fixed)
MK-886	Potent and specific inhibitor of leukotriene biosynthesis	10.0 (± 1.25)	23.5 (± 6.6)	≥ 30	-
L-162,313	AT1 angiotensin II receptor agonist	11.5 (± 1.99)	15.5 (± 12.5)	≥ 30	-
(Z)-Guggulsterone	Bile acid receptor (FRX) antagonist	11.9 (± 1.14)	0 (fixed)	≥ 30	-
PD98,059	Specific inhibitor of the activation of MAPKK	14.6 (± 5.97)	22.9 (± 23.3)	≥ 30	-
GBR-12909 dihydrochloride	Selective dopamine reuptake inhibitor	15.1 (± 1.16)	0 (fixed)	≥ 30	-
Rotlerin	PKC and CaM kinase III inhibitor	16.2 (± 10.9)	17.2 (± 42.4)	≥ 30	-
YC-1	NO-independent guanylyl cyclase activator	16.9 (± 1.03)	0 (fixed)	≥ 30	-
Nimodipine	Potent L-type Ca ²⁺ channel antagonist	17.5 (± 3.02)	0 (fixed)	≥ 30	-
(R)-(+)-WIN 55,212-2 mesylate	High affinity cannabinoid receptor agonist	17.8 (± 10.7)	25.6 (± 28.3)	≥ 30	-
Dihydro-beta-erythroidine hydrobromide	Competitive nicotinic acetylcholine receptor antagonist	18.8 (± 1.08)	0 (fixed)	73.8 (± 20.4)	0 (fixed)
Nitrendipine	Ca ²⁺ channel blocker; antihypertensive	19.8 (± 2.11)	0 (fixed)	≥ 30	-
K185	Melatonin receptor antagonist	21.8 (± 1.55)	0 (fixed)	≥ 30	-
Nicardipine hydrochloride	L-type Ca ²⁺ channel antagonist; antihypertensive	21.9 (± 1.6)	0 (fixed)	≥ 30	-
8-(3-Chlorostyryl)caffeine	Selective A _{2A} adenosine receptor antagonist	22.0 (± 1.09)	0 (fixed)	≥ 30	-
GW2974	Dual EGFR and ErbB-2 receptor tyrosine kinase inhibitor	26.6 (± 1.73)	0 (fixed)	50.1 (± 41.8)	0 (fixed)

Compound Name	Reported Biological Activity	K _{2p} ^{18.1} IC ₅₀ (μM)	K _{2p} ^{18.1} Minimum Activity (%)	K _{2p} ^{9.1} IC ₅₀ (μM)	K _{2p} ^{9.1} Minimum Activity (%)
Calmidazolium chloride	Potent inhibitor of calmodulin activation of phosphodiesterase	27.9 (± 3.02)	0 (fixed)	≥ 30	-

IC₅₀ and minimum activity were calculated using Origin 6. When necessary, minimum activity values were fixed at 0 as indicated to allow calculation of IC₅₀. Numbers in parentheses indicate error values as determined by the software. Dashes represent lack of compound activity.

Table 2

Potency and Efficacy Values from Validation Assay for Validated K_{2p}18.1 Activators

Compound Name	Reported Biological Activity	K _{2p} 18.1 EC ₅₀ (μM)	K _{2p} 18.1 Maximum Activity (%)	K _{2p} 9.1 EC ₅₀ (μM)	K _{2p} 9.1 Maximum Activity (%)
(+)-cis-Dioxolane iodide	Muscarinic acetylcholine receptor agonist	0.04 (± 0.01)	165 (± 3.00)	≥ 30	-
OXA-22 Iodide	Muscarinic acetylcholine receptor agonist	0.06 (± 0.01)	166 (± 4.50)	≥ 30	-
Oxotremorine Methiodide	Muscarinic acetylcholine receptor agonist	0.24 (± 0.02)	171 (± 4.60)	≥ 30	-
Acetyl-beta-methylcholine chloride	M1 muscarinic acetylcholine receptor agonist	0.65 (± 0.10)	184 (± 2.38)	≥ 30	-
Carbachol	Acetylcholine receptor agonist	1.59 (± 0.45)	190 (± 9.96)	≥ 30	-
Arecoline hydrobromide	Acetylcholine receptor agonist	2.70 (± 1.58)	155 (± 10.8)	≥ 30	-
Sipiperone Hydrochloride	D2 dopamine receptor antagonist	3.02 (± 0.83)	161 (± 4.90)	≥ 30	-
Phorbol 12-myristate 13-acetate	Activates PKC	0.03 (± 0.02)	130 (± 2.01)	≥ 30	-

EC₅₀ and maximum activity were calculated using Origin 6. Numbers in parentheses indicate error values as determined by the software. Dashes represent lack of compound activity.